ISSN 0915-633X

NATIONAL INSTITUTE FOR FUSION SCIENCE

Decay Process of a Magnetic Island by Forced Reconnection

K. Nagasaki and K. Itoh

(Received – Feb. 8, 1991)

NIFS-80 Mar. 1991

RESEARCH REPORT
NIFS Series

NAGOYA, JAPAN

Decay Process of a Magnetic Island by Forced Reconnection

K. Nagasaki and K. Itoh†

Plasma Physics Laboratory, Kyoto University
Gokasho, Uji, Kyoto 611, Japan
† *National Institute for Fusion Science*
Chikusaku, Nagoya 464-01, Japan

Abstract

Time evolution of a magnetic island by forced reconnection, especially the decay process is analyzed. A simple slab model is used and the magnetic island is considered to have a single helicity. The plasma is assumed to be incompressible. The evolution time is affected by the presence of an original magnetic island. In the decay process, a current flows along the separatrix of the magnetic island, and the current layer width depends on the magnetic island width, when the island is relatively wide compared to the current layer. In the presence of a magnetic island, even if the magnetic Reynolds number S increases, the current layer does not become narrower. This leads to the slow evolution of the magnetic island. It is found that the time scale $S^1\tau_A$ is required to reach the last equilibrium regardless of the nonlinear terms. This is slower than that of the growth process, $S^{3/5}\tau_A$.

KEYWORDS: magnetic island, forced reconnection, decay process

1 Introduction

In toroidal plasmas, an equilibrium in which all the magnetic surfaces are nested tori could exist if there were no perturbations. Actually, however, some of the magnetic surfaces are not nested due to MHD fluctuations and error fields, etc. When the boundary in the symmetric equilibrium state, which is defined as equilibrium (I), is perturbed so as to resonate a rational magnetic surface, the system evolves into another equilibrium. This equilibrium has two classes of solution. The first class of equilibrium has a surface current and a finite magnetic field jump on the resonant surface. There is no topological change of the magnetic surfaces. This equilibrium exists in the ideal MHD state where the resistivity does not play an important role in the magnetic reconnection. The second class of equilibrium has a topological change and no surface current, resulting in the presence of magnetic islands on the resonant surface. We define the first class as equilibrium (II), and the second class as (III). Actually, the plasma cannot stay long in (II) before evolving into (III), because the plasma has a finite resistivity. We shall call this time evolution the growth process. The growth process brought about by forced reconnection was analytically studied by Hahm and Kulsrud[1].

Next, suppose that the boundary condition reverts from the state in which the island exists on the resonant surface to the original symmetric state. The system will then evolve to another equilibrium. As in the growth process, there are two classes of equilibrium. The first has no topological change; there is still a magnetic island on the resonant surface. We define this equilibrium as (IV). The second has a topological change; the island disappears and the system returns to its original symmetric equilibrium (I). We shall call the time evolution from (IV) to (I) the decay process. The question is whether or not the decay process is different from the growth process. In this article, we will analyze the decay process and show what the difference is between the growth process and the decay process.

The problem of magnetic reconnection has been widely studied during the past

many years. Historically, there are two major models for steady state reconnection: one by Sweet[2] and Parker[3], and the other by Petschek[4]. There also exist numerical simulation studies [5]–[8]. They discussed about the driven reconnection in which the plasma flow to the neutral layer is important. However, when the magnetic island in the confined laboratory plasma are controlled by adding the external coil current, the effect of the plasma flow on the reconnection rate is weak. Instead the reconnection is strongly affected by the flux perturbation. In the same way of ref.[1], the island evolution by forced reconnection in which the boundary flux is perturbed is investigated.

Control of the magnetic island in tokamaks has been studied experimentally[9][10] and theoretically[11][12]. Other researchers have estimated the time evolution of magnetic islands, e.g., the response of magnetic islands to external perturbations, the necessary time for active feedback control and the matching between the island and the perturbation phases, etc., from the technological viewpoint. In this paper, we will study the time evolution of the magnetic island from the viewpoint of the physical mechanism. The plasma flow and the current density profile near the separatrix, which have a relation to the magnetic reconnection of field lines, are analyzed in detail.

A simple slab model is used and the magnetic island is assumed to have only a single helicity. In toroidal magnetic confinement systems such as tokamaks and torsatron/heliotron, fusion plasmas have a low beta and a small kinetic energy. Therefore they can be considered to be incompressible . The stationary plasma flow from the exterior region is not considered and only the flux is perturbed at the boundary. Reduced resistive MHD equations are solved to evaluate the time evolution of the magnetic island. The equations are calculated numerically and can be estimated analytically only in the ideal MHD phase.

In Sec. 2, geometry and basic equations are described. In Sec. 3, the growth process is reviewed. The decay process is studied in Sec. 4. The analytical solution of the flux function in the ideal MHD phase is described and numerical results are shown. The effect of the magnetic island on reconnection is discussed. Summary and discussions can be found in Sec.4.

2 Geometry and Basic equations

To analyze the growth and decay process, a simple geometry is used as shown in Fig. 1. The plasma is assumed to be incompressible and surrounded by the conducting wall at the boundary $x = \pm a$. The magnetic field has a uniform gradient in the x-direction and no z-dependence. The equilibrium magnetic field is given as

$$\mathbf{B} = B_z \nabla z + B_{y0} \frac{x}{a} \nabla y, \tag{2.1}$$

where B_{y0} and B_z are constant. By introducing the flux function ψ, the magnetic field can be written as

$$\mathbf{B} = B_z \nabla z + \nabla z \times \nabla \psi. \tag{2.2}$$

When the boundary is perturbed, the system evolves into a new equilibrium. The resistive MHD equations are solved to analyze the time evolution of a magnetic island. The resistive MHD equations are described as

$$\left.\begin{aligned} \rho \frac{d\mathbf{v}}{dt} &= \mathbf{J} \times \mathbf{B} - \nabla p \\ \frac{\partial \mathbf{B}}{\partial t} &= -\nabla \times \mathbf{E} \\ \mathbf{E} + \mathbf{v} \times \mathbf{B} &= \eta \mathbf{J} \\ 4\pi \mathbf{J} &= \nabla \times \mathbf{B} \end{aligned}\right\} \tag{2.3}$$

where $\rho, p, \mathbf{v}, \mathbf{J}, \mathbf{E}$ are mass density, plasma pressure, flow velocity, current density and electric field, respectively. By introducing the stream function ϕ and the vorticity U as

$$\left.\begin{aligned} \mathbf{v} &= \nabla z \times \nabla \phi \\ U &= \nabla^2 \phi, \end{aligned}\right\} \tag{2.4}$$

the reduced MHD equations for ψ and ϕ are written as [13]

$$\left.\begin{aligned} &\frac{\partial \psi}{\partial t} + \nabla z \times \nabla \phi \cdot \nabla \psi = \eta J \\ &\rho \left(\frac{\partial U}{\partial t} + \nabla z \times \nabla \phi \cdot \nabla U \right) = \nabla z \times \nabla \psi \cdot \nabla J \\ &J = \frac{1}{4\pi} \nabla^2 \psi \\ &U = \nabla^2 \phi, \end{aligned}\right\} \tag{2.5}$$

where J is the z-component of the current density.

When the boundary perturbation amplitude δ is small compared to a, $\delta/a \ll 1$, the quantities in eq.(2.5) are approximated by

$$\left.\begin{aligned} \psi &= \psi_0 + \psi_1 \\ \phi &= \phi_1 \\ J &= J_0 + J_1 \\ U &= U_1, \end{aligned}\right\} \tag{2.6}$$

where sub 0 and 1 denote the original equilibrium terms and the perturbed terms, respectively. We solve the time evolution of the first order terms from the first equilibrium to the second one by using eqs.(2.5) and (2.6).

3 Growth Process

Hahm and Kulsrud analytically studied the growth process and indicated the time scale of the evolution in both linear and nonlinear cases. Here analysis of the growth process is reviewed in brief.

When the boundary is perturbed as

$$x = \pm(a - \delta \cos ky), \tag{3.1}$$

the system evolves into a new equilibrium to the first order in δ. When the boundary is perturbed as (3.1), the flux function is given by

$$\psi = \psi_0 + \psi_1(x) \cos ky, \tag{3.2}$$

where $\psi_0 = (B_{y0}/2a)x^2$. The equation for the first order quantity $\psi_1(x)$ is obtained by substituting eq.(3.2) into the force balance equation $\mathbf{B} \cdot \nabla \mathbf{J} = 0$ as

$$\frac{B_{y0}}{a} x (\frac{\partial^2}{\partial x^2}\psi_1 - k^2 \psi_1) = 0. \tag{3.3}$$

Equation (3.3) is solved by making use of the boundary condition $\psi_1(a) = B_{y0}\delta$ as

$$\psi_1(x) = \psi_1(0)(\cosh kx - \frac{\sinh kx}{\tanh ka}) + B_{y0}\delta \frac{\sinh kx}{\sinh ka}. \tag{3.4}$$

The central value $\psi_1(0)$ has two solutions, $\psi_1(0) = 0$ and $B_{y0}\delta/\cosh ka$. The former corresponds to the equilibrium (II), the latter to the equilibrium (III). Island width Δ depends on the amplitude of perturbations at the boundary as shown in the expression $4\sqrt{a\psi_1(0)/B_{y0}}$.

By considering the y-dependence of ψ, we may write the stream function ϕ during the time evolution in the following form,

$$\phi = \phi_1(x) \sin ky. \tag{3.5}$$

The flux value $\psi_1(0)$ evolves from 0 to $B_{y0}\delta/\cosh ka$. The time stage is divided into four phases, (A) ideal MHD, (B) transition from ideal MHD to resistive MHD, (C)

resistive MHD and (D)constant ψ phases. These phases are characterized by the order of time $S^{\alpha}\tau_A$ $(0 \leq \alpha \leq 1)$, where S is magnetic Reynolds number and τ_A is poloidal Alfven time.

When the perturbation is small, $\delta/a \ll (\tau_A/\tau_R)^{4/5}$, the linear treatment is possible. If $t \ll S^{1/3}\tau_A$, the time stage is phase (B). The plasma flows are given by the ideal MHD theory. For $t \sim S^{1/3}\tau_A$, the full theory of phase (C) applies. The resistivity begins to reconnect the magnetic field lines. For $S^{1/3}\tau_A \ll t \ll S^{3/5}\tau_A$, the constant ψ approximation in phase (D) applies, and the small ka theory $(ka \sim 1)$ is applicable.[14]. For $t \sim S^{3/5}\tau_A$, the flux $\psi_1(0)$ has a second equilibrium value, which it reaches only after overshooting. This means that the tearing time scale $S^{3/5}\tau_A$ is necessary to reach the equilibrium (III).

When the magnetic island has a size comparable with the resistive layer, the nonlinear effect should be considered.[15] Since a sizable nonlinear eddy current arises, producing $\mathbf{J} \times \mathbf{B}$ forces which oppose the flow pattern, the exponential growth is replaced by algebraic growth on a much slower time scale. Reconnection and the island growth occur on the nonlinear time scale $\tau_{NL} \sim (\delta/a)^{1/2}\tau_R$. The overshooting of the magnetic island does not occur.

4 Decay Process

4.1 Analytical Estimation

On evaluating the decay process, we will make use of the reduced MHD equations again. The equilibrium term is different from that in the growth process. The equilibrium flux function should be changed as follows,

$$\psi_{eq} = \psi_0 + B_{y0}\delta\frac{\cosh kx}{\cosh ka}\cos ky. \tag{4.1}$$

The second term in eq.(4.1) is related to the original magnetic island. The decay process is expected to evolve in a different way when the original island width is not negligible.

In the decay process, an analytical estimate can be obtained only in the ideal MHD phase. Following the coordinates (ψ, ζ, z) rather than the Cartesian coordinates is convenient.

$$\left.\begin{aligned} \psi &= \frac{B_{y0}}{2a}x^2 + \psi_s \cosh kx \cos ky \\ \nabla\zeta &= \frac{4B_{y0}}{4B_{y0} + k^2 a\psi_s}\frac{\nabla z \times \nabla\psi}{\mid \nabla\psi \mid} \\ z &= z \end{aligned}\right\} \tag{4.2}$$

where $\psi_s = B_{y0}\delta/\cosh ka$. The component ψ represents the flux surface with a magnetic island and the component ζ is perpendicular to both ψ and z. Using these coordinates, we can deduce the equation for the time dependent perturbed flux function $\tilde{\psi}$ as

$$\frac{4\pi\rho}{k^2}(\frac{4B_{y0} + k^2 a\psi_s}{4B_{y0}})^2\frac{\partial^2}{\partial t^2}\nabla^2\frac{\tilde{\psi}}{\mid \nabla\psi \mid} = -\mid \nabla\psi \mid \nabla^2\tilde{\psi}. \tag{4.3}$$

We approximate $\mid \nabla\psi \mid$ as

$$\mid \nabla\upsilon \mid^2 \sim (\frac{B_{y0}}{a} + k^2\psi_s \cos ky)^2 + (k\psi_s \sin ky)^2. \tag{4.4}$$

Using $x^2 \sim (2a/B_{y0})(\psi - \psi_s \cos ky)$, we have

$$\mid \nabla\psi \mid^2 \sim \sqrt{\frac{2B_{y0}\psi}{a}}. \tag{4.5}$$

When the Laplacian is approximated as $\nabla^2 \sim (B_{y0}/2)(2\psi\partial^2/\partial\psi^2 + \partial/\partial\psi)$, eq.(4.3) can be rewritten as

$$\frac{4\pi\rho}{k^2}\left(\frac{4B_{y0}+k^2a\psi_s}{4B_{y0}}\right)^2\frac{\partial^2}{\partial t^2}\frac{\partial^2}{\partial u^2}\frac{\tilde{\psi}}{u} = -u\frac{\partial^2}{\partial u^2}\tilde{\psi} \tag{4.6}$$

where $u \equiv \sqrt{\psi}$. This equation is solved by the same methods in ref.[1] and we have

$$\tilde{\psi} \simeq C_1 u \int_0^{hut/\tau_A} dv \frac{\sin v}{v}, \tag{4.7}$$

where $h = 4k\sqrt{aB_{y0}}/(4B_{y0} + k^2a\psi_s)$ and C_1 is constant. Since the perturbed flux function in the ideal MHD phase of the growth process is written as[1]

$$\psi_1 \simeq C_2 x \int_0^{\frac{kx_1}{\tau_A}} dv \frac{\sin v}{v}, \tag{4.8}$$

it is found that eqs. (4.7) and (4.8) have an analogous form. The perturbed flux is distributed according to the background equilibrium flux profile.

In the ideal MHD phase, there is almost no difference in the time evolution of $\psi_1(0)$ between the growth process and the decay process. However, the plasma flow and the current density profile are quite different. In the growth process, the plasma mainly flows along the $x = 0$ axis and the current has a large gradient around $x = 0$. On the other hand, in the decay process, since the current density has a large gradient at the X-point of the separatrix and it is distributed according to the background flux, it has a gradient at the separatrix. The time dependent perturbed stream function $\tilde{\phi}$ is obtained by solving the following equation:

$$4\pi\rho\frac{\partial^2}{\partial t^2}\nabla^2\tilde{\phi} = f(\nabla\zeta\cdot\nabla)\nabla^2(f\nabla\cdot\nabla\tilde{\phi}) \tag{4.9}$$

where $f = (4B_{y0} + k^2a\psi_s) \mid \nabla\psi \mid /(16\pi B_{y0})$. Since this equation indicates that the stream function is also distributed according to the background flux, the plasma mainly flows along the separatrix.

In the resistive time scale $t \gg S^{1/3}\tau_A$, we must consider the effect of the resistive term which is difficult to estimate analytically. In Sec. 4.2, we will show the numerical method and the results.

4.2 Numerical Results

4.2.1 Numerical Methods

The Cartesian coordinates are used in numerical calculations. With these coordinates, higher Fourier modes coupled with the island term in equilibrium quantities should be considered. Perturbed quantities are written as

$$\left.\begin{aligned}
\tilde{\psi} &= \sum_{j=0} \tilde{\psi}_j \cos jky \\
\tilde{\phi} &= \sum_{j=1} \tilde{\phi}_j \sin jky \\
\tilde{J} &= \sum_{j=0} \tilde{J}_j \cos jky \\
\tilde{U} &= \sum_{j=1} \tilde{U}_j \sin jky.
\end{aligned}\right\} \tag{4.10}$$

Substituting (4.1) and (4.10) into (2.5), we can obtain the equations for each modes. After setting up the perturbation, the boundary conditions are given as

$$\left.\begin{aligned}
\tilde{\psi}_j(x = \pm a) &= \begin{cases} -B_{y0}\delta & (j = 1) \\ 0 & (j \neq 1) \end{cases} \\
\tilde{\phi}_j(x = \pm a) &= 0.
\end{aligned}\right\} \tag{4.11}$$

The symmetry $\tilde{\psi}(x) = \tilde{\psi}(-x), \tilde{\phi}(x) = -\tilde{\phi}(-x)$ makes it possible to reduce the region $0 \leq x \leq a$. The estimate of the numerical error is given in Appendix.

4.2.2 Example

Figure 2 shows the evolution of the flux function $\tilde{\psi}$. Parameters are chosen as $S = 10^5, \delta/a = 10^{-2}$ and $ak = 1$. Both growth and decay processes are plotted. The overshooting phenomena can be seen in the growth process in the absence of the nonlinear terms, which agree with the analytical estimate in Sec. 3. The decay process is slower than the growth one. This delay becomes large with the increase of S. Furthermore we should note the effect of the nonlinear terms, $\nabla z \times \nabla\tilde{\phi} \cdot \nabla\tilde{\psi}, \nabla z \times \nabla\tilde{\phi} \cdot \nabla\tilde{U}$ and $\nabla z \times \nabla\tilde{\psi} \cdot \nabla\tilde{J}$. In the growth process, when the magnetic island grows larger than

the resistive layer, nonlinear eddy current becomes more pronounced, producing the $J \times B$ force opposing the fluid flow pattern. This physical mechanism leads to a slower time evolution of the magnetic island. This means that the nonlinear terms play an important role in the growth process. In the decay process, on the other hand, the evolution hardly changes regardless of the nonlinear terms as seen in Fig. 2. This implies that other mechanism dominates the island evolution. It is also confirmed that the current profile near the rational surface does not change. In the next subsection, we will explain why the decay process evolves slower. The nonlinear terms are neglected. This approximation shortens the calculation time.

4.2.3 Effect of the Magnetic Island

In the decay process, the plasma mainly flows along the separatrix and the current density has a large gradient there. This means that the island has an influence on its own evolution. Figure 3 shows the example contours of flux function, current density and stream function. The geometry of the magnetic surface affects the current density profile. We note that the current profile near the X-point is still important because the current density is peaked at the X-point. Figure 4 shows the time evolution of the current density at both the X- and O-points of the separatrix. The magnetic Reynolds number chosen is $S = 10^5$. During the ideal MHD phase, the current density increases as in the growth process, but it is suppressed during the resistive MHD phase. Since the reconnection rate of field lines is determined by the current intensity at the X-point, smaller current intensity slows down the time evolution. Figure 5 shows the dependence of the current layer width in the $x-$ direction on the $y = 0$ plane, Δ_x, and that in the $y-$ direction on the $x = 0$ plane, Δ_y, and the current intensity at the X-point, $\tilde{J}(0)$. In the growth process, analytical estimate gives us that $\tilde{J}(0)$, Δ_x and Δ_y scale as $S^{1/3}$, $S^{-1/3}$ and S^0, respectively. In the decay process, when S is small, Δ_x is wider than the island width, and $\tilde{J}(0)$, Δ_x scale like in the growth process. However, as S increases, $\tilde{J}(0)$, Δ_x and Δ_y become independent of S. This indicates that the current density at the X-point is determined not by the Reynolds number but by the

magnetic geometry when the current layer width in the x-direction is relatively narrow compared to the island width.

Our result $\Delta_x < \Delta_y$ differs from that of ref.[6]. This is because the external flow is weak in our model. In ref.[6], there are strong external flow along the y-axis ($v \sim v_A$) and the magnetic surfaces near the X-point are modified. The angle θ between the x-axis and magnetic surace is nearly zero and v_x is larger than v_y. From the relation of $\nabla \cdot \mathbf{v} = 0$, we have $v_x/\Delta_x \simeq v_y/\Delta_y$. (The left term is not strictly equal to the right one, because they are measured at the different points.) These results lead to $\Delta_x > \Delta_y$. In our model, on the other hand, the external flow is weak and the magnetic surfaces are weakly changed as seen in Fig.3(a). For example, when parameters are $S = 10^4, \delta/a = 10^{-2}, t/\tau_A = 100$, the maximum velocity is $v/v_A \sim 3.6 \times 10^{-3}$. The angle θ is larger than $\pi/4$, and the maximum of v_x is smaller than that of v_y. As a result, we obtain that Δ_x is smaller than Δ_y.

The current density oscillates in the time evolution as shown in Fig. 4. This phenomenon occurs only in the decay process. Figure 6 shows the time history of the current density contours at one oscillation period. The wave which has a wave length $\lambda = 2\pi\tau_A/(kt)$ is enhanced by perturbing the boundary. Though it moves to the slab center, it cannot enter into the original island, resulting in the negative current layer at the separatrix. When the layer width becomes thin and reaches a critical value which scales as $\Delta \sim (t/S)^{1/2}$, the current diffuses and the wave front structure is broken. Since the width scales as $1/t$, this relation predicts that the time scale of the relaxation phenomena is given as $S^{1/3}$. This relaxation makes the current profile level down, and the current peaking is relaxed to almost zero. When the next wave reaches to the separatrix, the negative current layer is constructed again. In the growth process, on the contrary, the current on the island is not peaked in the resistive phase, except in the vicinity of the X-point. The merging of the skin current on the separatrix and the outer oscillating current does not take place and the oscillation process does not occur in the growth process.

The S-dependence of evolution time is shown in Fig. 7. The time it takes for

island width to decrease by half is plotted. In the growth process, this time scales to the tearing time $S^{3/5}\tau_A$ as expected in Sec. 2. It is found that in the decay process, it scales as $t \sim (1/20)S^1\tau_A$ at $ak = 1, \delta k = 10^{-2}$. This indicates that the resistive diffusion time is necessary for the system to reach the last equilibrium even in the linear case. The reason is that the current density at the X-point has an upper limit, which is weakly dependent on the magnetic Reynolds number. Since the growth rate in the resistive MHD phase is approximated as $1/\tau \propto \eta J$, we can obtain $\tau \propto S$.

From above results, it is found that the evolution time in the decay process depends not only on S, but also on the island width. For a given S, the relationship between the evolution time and the island width is shown in Fig. 8. S is fixed at 10^5. When the original magnetic island is smaller than the current layer, the time evolution is similar to that of the growth process. This is because the existence of the island is "hidden" in the current layer. When the original island is wide compared to the current layer, the island effect appears.

5 Summary and Discussion

The time evolution of the magnetic island by forced reconnection was investigated in the slab geometry. In the equilibrium where the plasma has a magnetic island (III), the boundary is perturbed so that the island may disappear. The decay process evolves in a different way from the growth process. The plasma behavior strongly depends on the magnetic island, i.e., the plasma mainly flows along the separatrix and the current density has a large gradient near the separatrix. The peaking of the perturbed current near the X-point is suppressed by the parallel resistivity and the existence of the magnetic island.

If the resistivity is large and the thickness of the current layer governed by η is large compared to the original island width, the existence of the island has little effect on the development of the current at the X-point. On the other hand, if S becomes large, the width of current density layer weakly depends on S and has a characteristic value so that the current density value at the X-point has an upper limit. This leads to a slower time evolution of the magnetic island. It was found that a longer time scale than $S^{3/5}\tau_A$, namely $S^1\tau_A$ is necessary to reach the last equilibrium even by neglecting the nonlinear terms. If the boundary is controlled so as to make the magnetic island disappear, we should consider that it takes a period of time which depend on the magnetic island size.

The reduced MHD equations can also be solved in the cylindrical geometry and the mechanism of the system would likely not be changed. However, if the toroidal effect is included, consideration may be given to the overlapping of multi-islands, which causes the magnetic fields to become stochastic. The randomness of the field lines rapidly diffuses the current in a radial manner, possibly resulting in a slower time evolution. This problem may play important roles in recent edge-ergodization experiments in which multi-helicity magnetic perturbations are imposed on tokamak plasmas.[16]–[18] The effect of the stochasticity will be studied in the forthcoming work.

The perturbation at the boundary is rapidly set up on the MHD time scale. This

boundary control is possible, but in real systems more set up time may be necessary. We also determine the effect of the set up time on the time evolution. The result is that if the set up time is within the limits of the ideal MHD phase ($S^{1/3}\tau_A$), the time necessary to reach the equilibrium is not greatly affected and the $S^1\tau_A$ property is not changed. Since real set up time can be set to less than $S^{1/3}\tau_A$, the model rapid set up time used in this article would be appropriate for real plasma analysis.

If the plasma kinetic energy is small, the plasma can be assumed to be incompressible. In general, the effect of the compressibility should be estimated. For example, in astronomical plasmas which have a large flow velocity, the compressibility can not be neglected in fast reconnection.[19][20] The resistive MHD equations applies only in low β, incompressible and large aspect ratio conditions.[13] If the compressibility is taken into account, the MHD equations must be solved directly and the calculation is likely to be complicated.

Acknowledgments

Authors wish to thank Dr. S.-I. Itoh and Dr. M. Yagi for helpful discussions. One of authors (K.N.) would like to thank Dr. Y. Nakamura and Dr. K. Ichiguchi for helping with the numerical calculations. Professor A. Iiyoshi's encouragement was also appreciated. This work was partly supported by the Grant-in-Aid for Fusion Research from the Ministry of Education, Science and Culture.

Appendix

In this appendix, the numerical methods and the numerical error are shown. Since the reconnection rate is strongly connected with the current density $\tilde{J}$ at the X-point of the separatrix, the relative error is estimated in terms of $\tilde{J}$. We carry out the spatial difference in the x-direction and the Fourier expansion in the y-direction. The mesh number in the x-direction and the mode number are defined as M_x and M_f, respectively. As for the time evolution, we employ two step algorithm. One Alfven time is devided by the mesh M_t.

Figure A.1 shows the relative error ε as a function of M_x. Parameters are $S = 5 \times 10^4, \delta/a = 10^{-2}, M_f = 50$, $M_t = 500$. and the evolution time is $t/\tau_A = 400$ ($\tilde{\psi}/\psi_s \simeq 0.25$). The relative error is given as $\varepsilon_x \propto M_x^{-4}$ because the fourth order central difference is done. Since we take $M_x = 500$ in this paper, the relative error is about 3×10^{-3}. As for the mesh M_t, the relative error is given as $\varepsilon_t \propto M_t^{-2}$ because of the second order explicit method. Figure A.2 shows the M_f dependence of ε_f. Parameters are $S = 5 \times 10^4, \delta/a = 10^{-2}, M_x = 500$ and $M_t = 500$. We can see that the error decreases exponentially with the increase of M_f.

References

[1] T. S. Hahm and R. M. Kulsrud: Phys. Fluids, **28** (1985) 2412.

[2] P. A. Sweet: in *Electromagnetic Phenomena in Collisional Physics*, IAU Symposium No.6, edited by B. Lehnert (Cambridge University Press, London) (1958) p.123.

[3] E. N. Parker: J. Geophys. Res. **62** (1957) 509.

[4] H. E. Petschek: Proc. AAS-NASA Symposium on Physics of Solar Flares (NASA SP-50, Washington, D. C., 1964) p.425.

[5] B. V. Waddell, M. N. Rosenbluth, D. A. Monticello and R. B. White, Nucl. Fusion**16** (1976) 528.

[6] D. Biskamp and H. Welter: Phys. Rev. Lett. **44** (1980) 1069

[7] D. Biskamp: Phys. Letters **87A** (1982) 357

[8] M. Ugai and T. Tsuda: J. Plasma Phys. **17** (1977) 337

[9] K. Yamazaki, K. Kawahata, Y. Abe, R. Akiyama, T. Amano, R. Ando, Y. Hamada, S. Hirokura, K. Ida, E. Kako, O. Kaneko, Y. Kawasumi, S. Kitagawa, T. Kuroda, K. Masai, K. Matsuoka, A. Mohri, M. Mugishima, N. Noda, I. Ogawa, K. Ohkubo, Y. Oka, K. Sakurai, M. Sasao, K. Sato, K.N. Sato, S. Tanahashi, Y. Taniguchi, K. Toi and T. Watari: Proc. 5th Int. Conf. on *Plasma Physics and Controlled Nuclear Fusion*, Kyoto, 1986, (IAEA, Vienna, 1987) Vol.1, p.309

[10] J.J. Ellis, A.A. Howling, A.W. Morris and D.C. Robinson: Proc. 10th Int. Conf. on *Plasma Physics and Controlled Nuclear Fusion*, London, 1984, (IAEA, Vienna, 1985) Vol.1, p.363

[11] J.A. Holms, B.A. Carreras, H.R. Hicks, S.J. Lynch and B.V. Waddell: Nucl. Fusion **19** (1979) 1333

[12] T.C. Hender, D.C. Robinson and J.A. Snipes: Proc. 11th Int. Conf. on *Plasma Physics and Controlled Nuclear Fusion*, Kyoto, 1986, (IAEA, Vienna, 1987) Vol.1, p.291

[13] H.R. Strauss: Phys. Fluids, **19** (1976) 134

[14] H.P. Furth, J. Killeen and M.N. Rosenbluth: Phys. Fluids, **6** (1963) 459

[15] P.H. Rutherford: Phys. Fluids **6** (1973) 1903

[16] S.C. McCool, A.J. Wooton, A.Y. Aydemir, R.D. Bengtson, J.A. Boedo, R.V. Brabenec, D.L. Brower, J.S. DeGrassie, T.E. Evans, S.P. Fan, J.C. Foster, M.S. Foster, K.W. Gentle, Y.X. He, R.L. Hickcock, G.L. Jackson, S.K. Kim, M. Kotchenreuther, N.C. Luhmann, Jr., W.H. Miner, Jr., N. Ohyabu, D.M. Patterson, W.A. Peebles, P.E. Phillipes, T.L. Rhodes, B. Richards, C.P. Ritz, D.W. Ross, W.L. Rowan, P.M. Schoch, B.A. Smith, J.C. Wiley, X.H. Yu, S.B. Zheng: Nucl. Fusion **29** (1989) 547

[17] S.C. McCool, A.J. Wooton, M. Kotchenreuther, A.Y. Aydemir, R.V. Brabenec, J.S. DeGrassie, T.E. Evans, R.L. Hickcock, B. Richards, W.L. Rowan, P.M. Schoch: Nucl. Fusion **30** (1990) 167

[18] T. Shoji and JFT-2M Group: paper SaJ13 presented in Jpn. Phys. Soc. Meeting (Kagoshima, 1989)

[19] T. Sato and T. Hayashi: Phys. Fluids **22** (1979) 1189

[20] R.B. White: Rev. Mod. Phys. **58** (1986) 183

Figure Captions

Fig. 1

Slab geometry of the system.

Fig. 2

Time evolution of the flux function. Real lines correspond to full calculations and dotted lines correspond to the case of neglecting the nonlinear terms. Parameters are $\delta/a = 10^{-2}$ and $S = 10^5$.

Fig. 3

Contours of (a) flux function, (b) current density and (c) stream function. Parameters are $\delta/a = 10^{-2}, S = 10^4$ and $t = 100\tau_A$.

Fig. 4

Time evolution of the current density both in the growth and decay processes. Parameters are the same as in Fig. 2. Real and dashed lines correspond to the X-point and O-point, respectively. The dotted line denotes the growth process.

Fig. 5

Dependence of the current layer width and the current intensity at the X-point. Symbols $\circ, \Delta$ and $\Box$ correspond to $\tilde{J}/J_s$, $\Delta_x k$ and $\Delta_y k$. J_s is defined as $J_s = \psi_s k^2/4\pi$. These are the values at $\tilde{\psi}/\psi_s = 0.25$.

Fig. 6

Time history of the current contour. Each figure correspond to the point A, B, C, and D in Fig. 4. Real and dotted line denote the positive and negative value, respectively.

Fig. 7

S-dependence of the time it takes the magnetic island width to decrease by half. Real and dashed lines correspond to the decay and growth processes, respectively.

Fig. 8

The relationship between the equilibrium time and the island width. As the island width increases, the equilibrium time comes to depend on the island width, being proportional to S.

Fig. A.1

Numerical error as a function of the spatial mesh M_x.

Fig. A.2

Numerical error as a function of the Fourier number M_f.

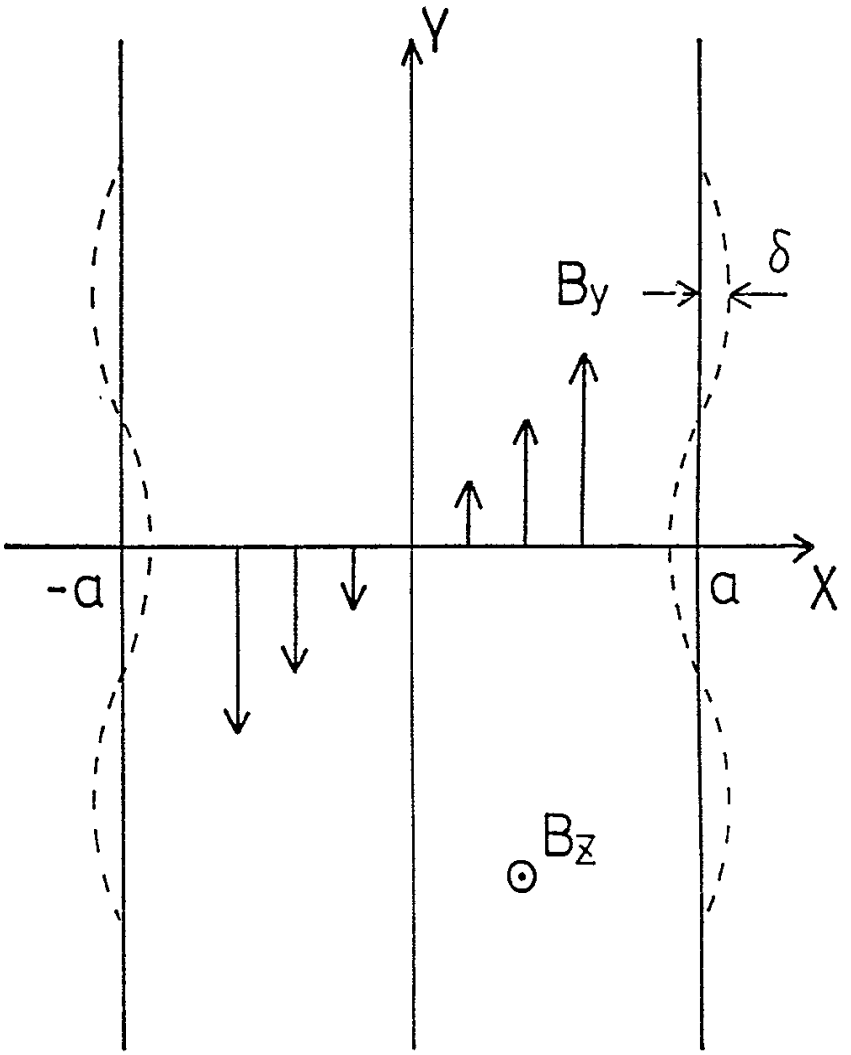

Fig. 1

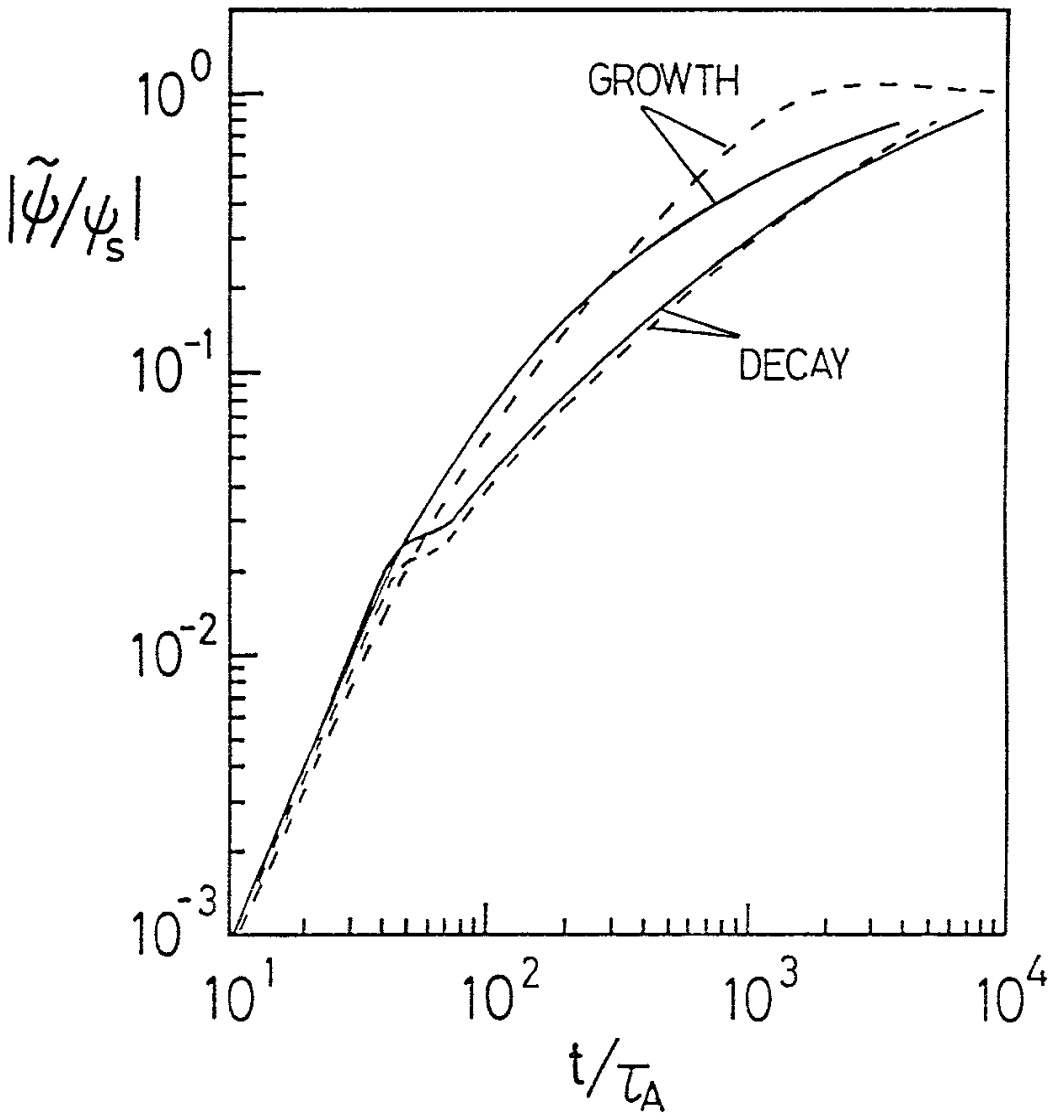
10^0
10^{-1}
10^{-2}
10^{-3}
$|\tilde{\psi}/\psi_s|$
GROWTH
DECAY
10^1
10^2
10^3
10^4
t/τ_A

Fig. 2

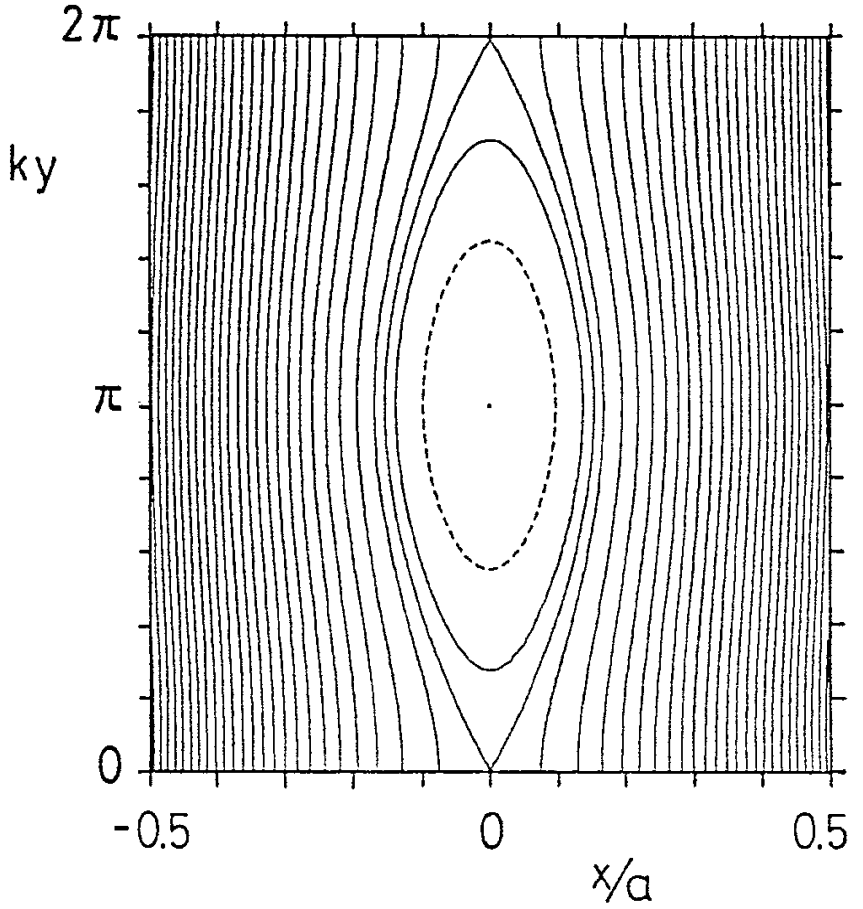

Fig. 3(a)

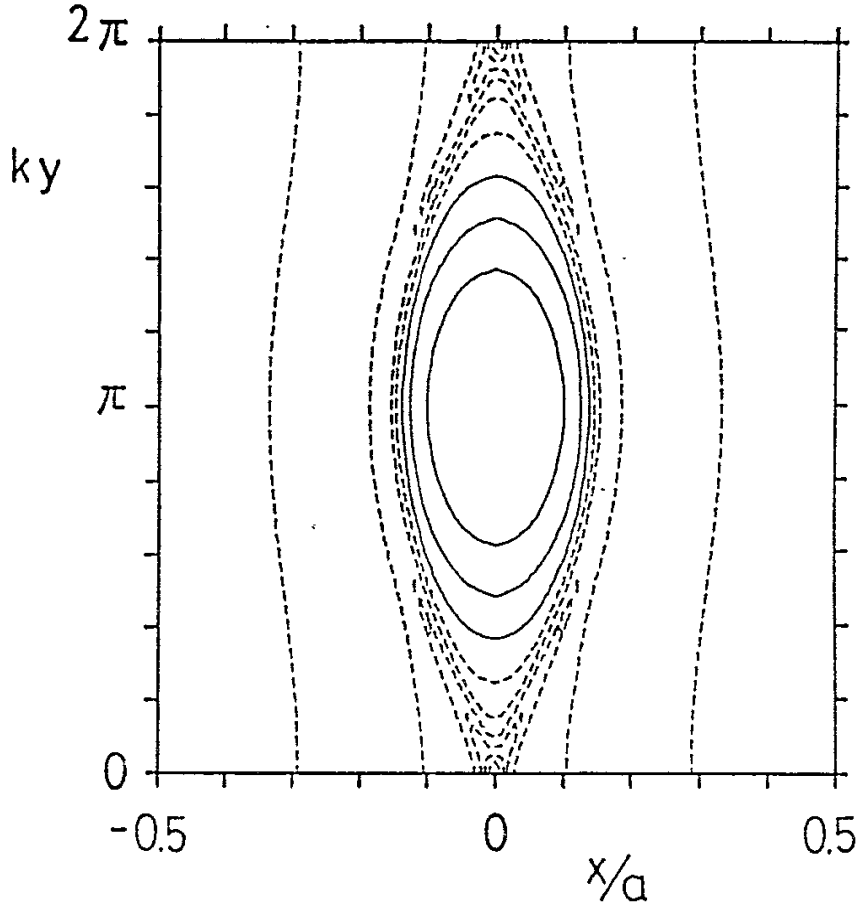

Fig. 3(b)

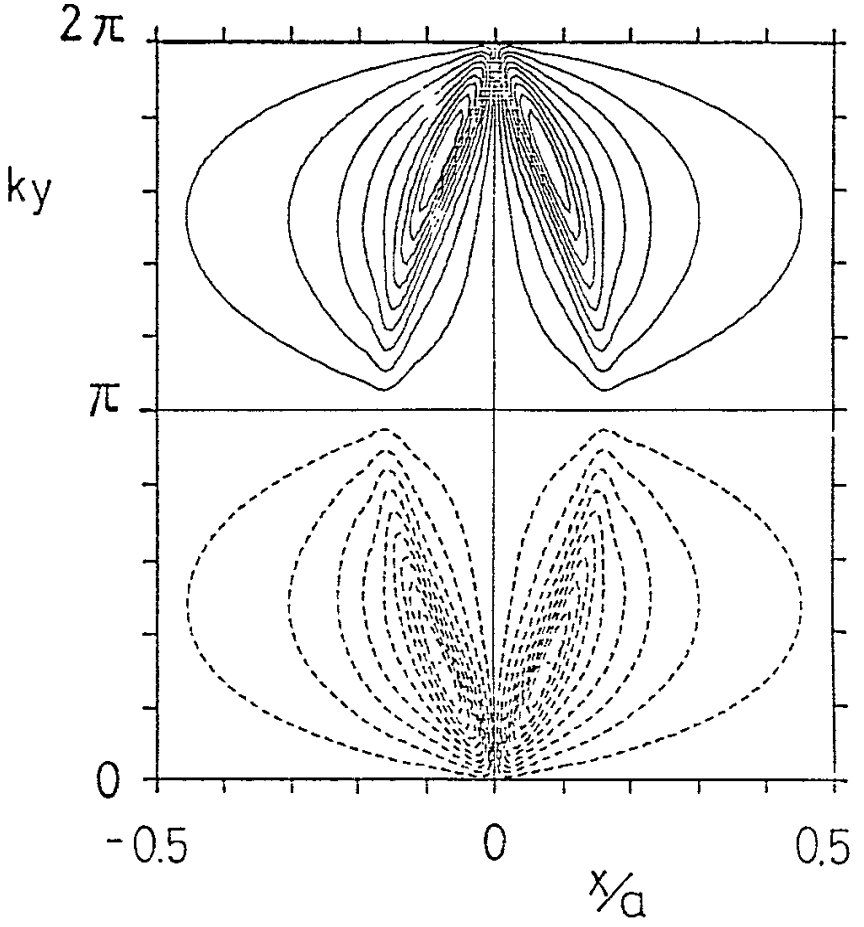

Fig. 3(c)

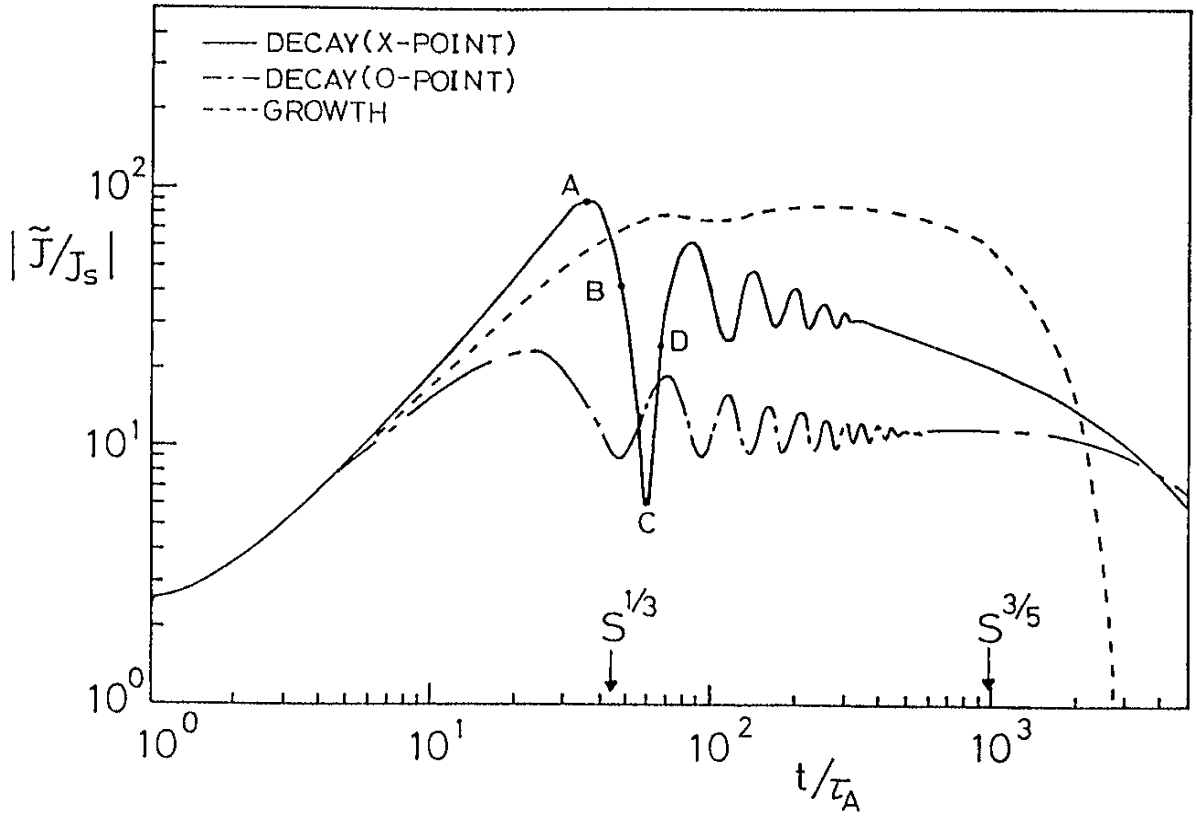
DECAY(X-POINT)
DECAY(O-POINT)
GROWTH
10^2
10^1
10^0
$|\tilde{J}/J_s|$
A
B
C
D
$S^{1/3}$
$S^{3/5}$
10^0
10^1
10^2
10^3
t/τ_A

Fig.4

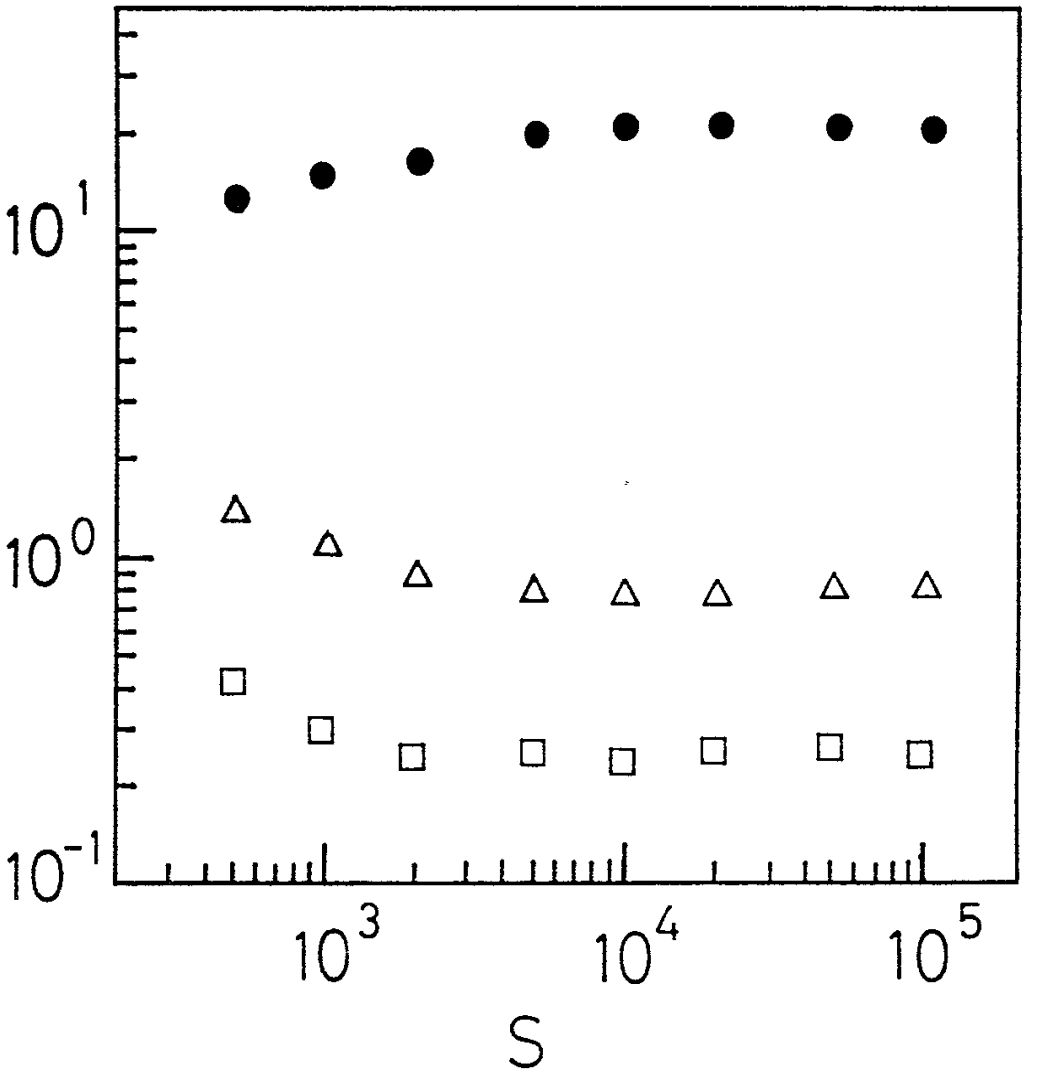

Fig. 5

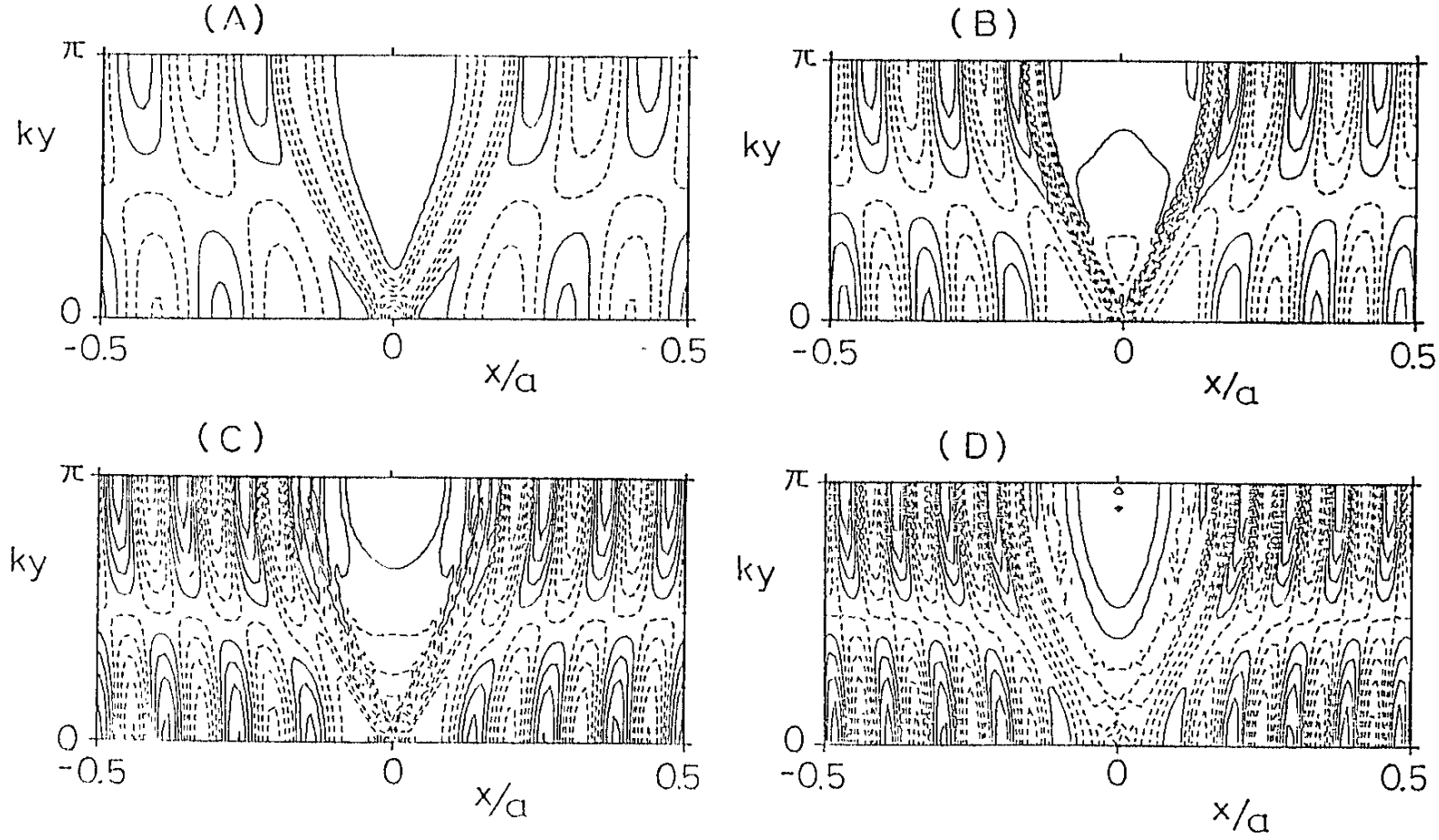

Fig. 6

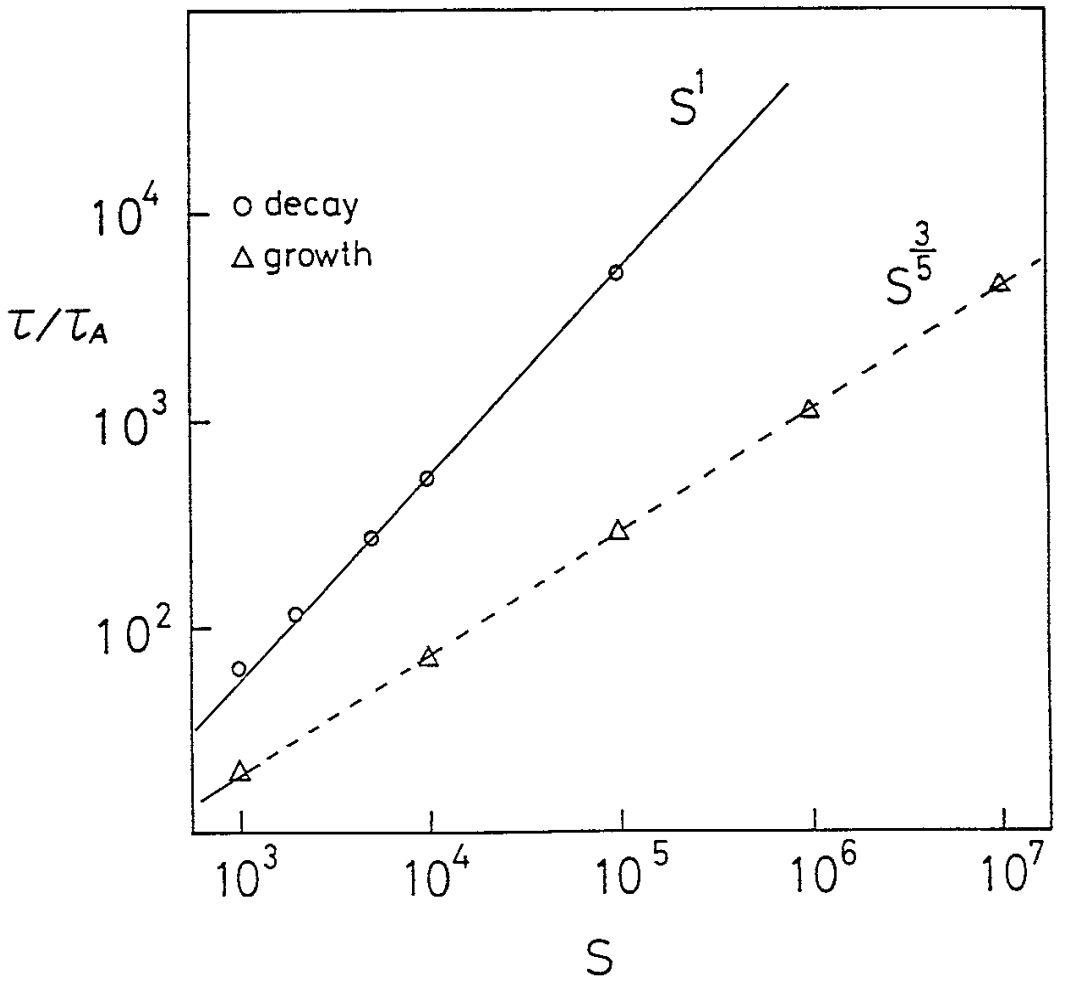
S^1
o decay
Δ growth
$S^{\frac{3}{5}}$
10^4
10^3
10^2
τ/τ_A
10^3
10^4
10^5
10^6
10^7
S

Fig. 7

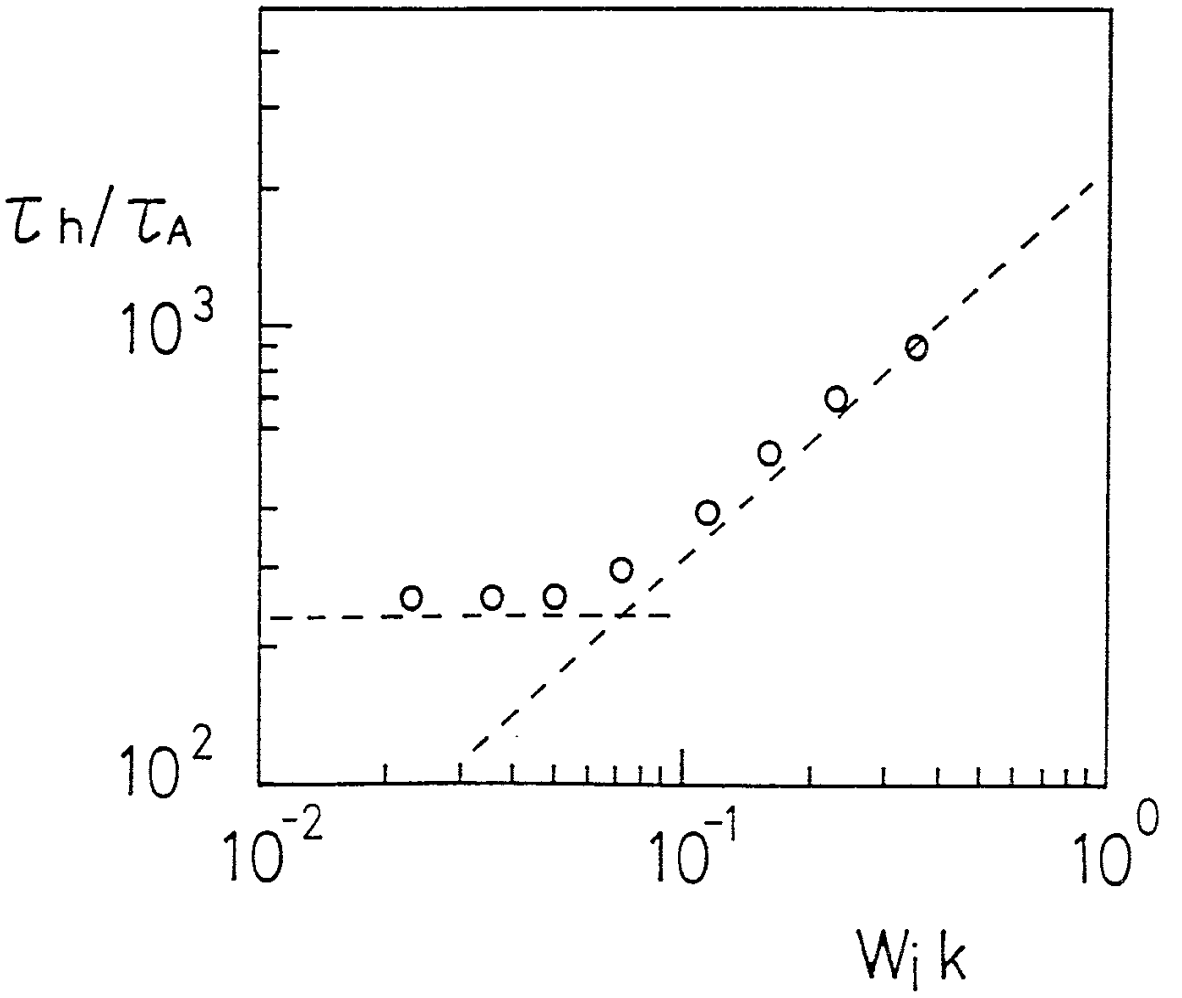

Fig. 8

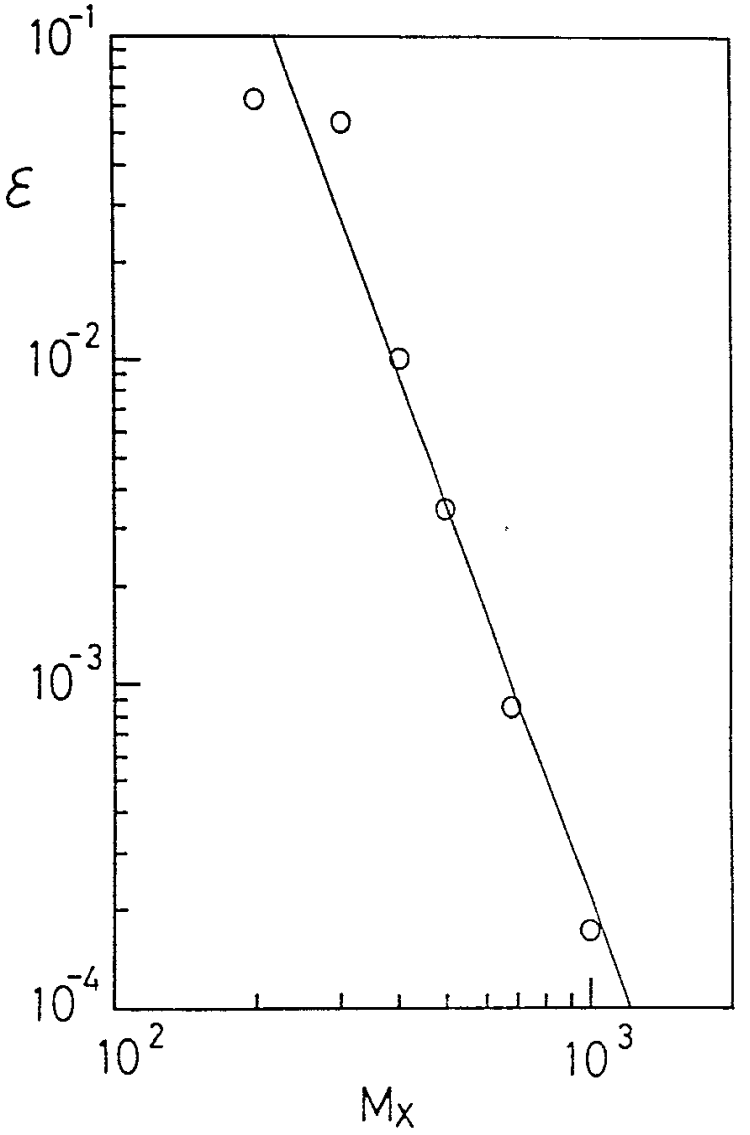

Fig. A1

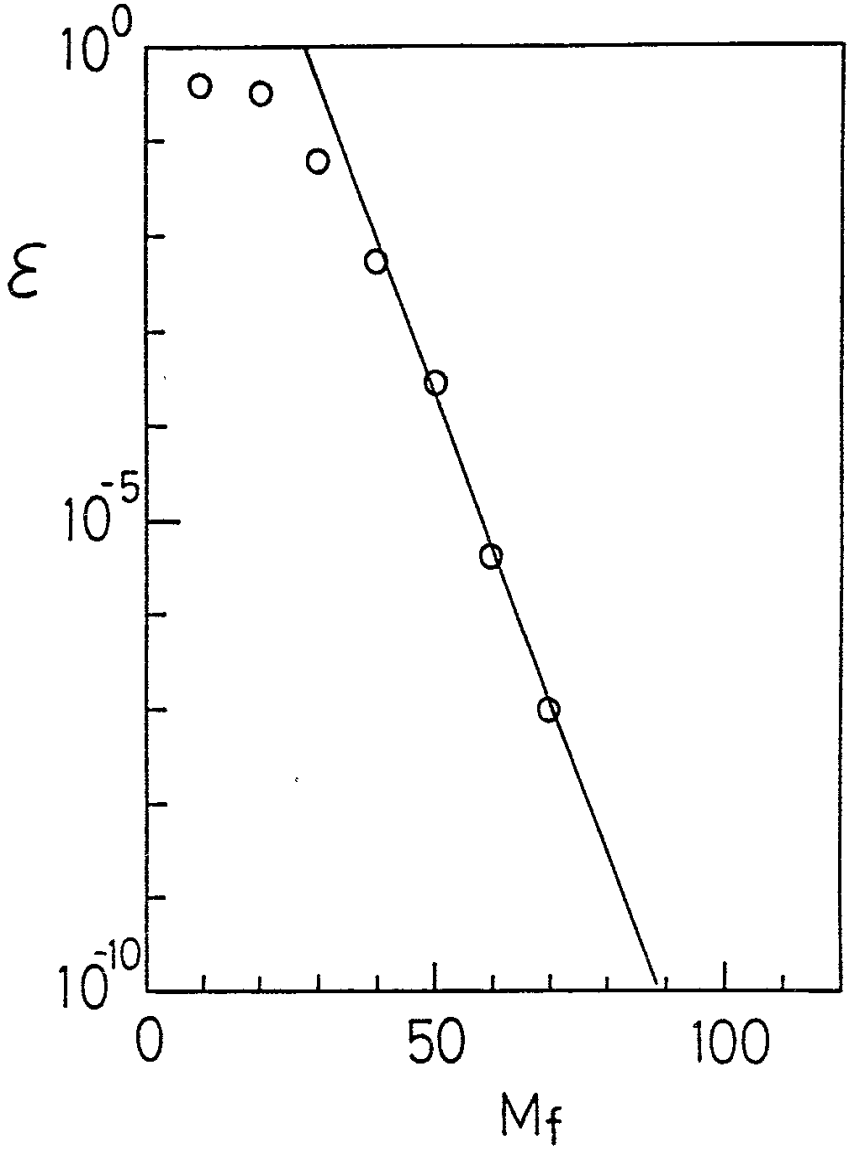

Fig. A 2

Recent Issues of NIFS Series

NIFS-30 K. Yamazaki, O. Motojima, M. Asao, M. Fujiwara and A. Iiyoshi, *Design Scalings and Optimizations for Super-Conducting Large Helical Devices* ; May 1990

NIFS-31 H. Sanuki, T. Kamimura, K. Hanatani, K. Itoh and J. Todoroki, *Effects of Electric Field on Particle Drift Orbits in a l =2 Torsatron* ; May 1990

NIFS-32 Yoshi H. Ichikawa, *Experiments and Applications of Soliton Physics*; June 1990

NIFS-33 S.-I. Itoh, *Anomalous Viscosity due to Drift Wave Turbulence* ; June 1990

NIFS-34 K. Hamamatsu, A. Fukuyama, S.-I. Itoh, K. Itoh and M. Azumi, *RF Helicity Injection and Current Drive* ; July 1990

NIFS-35 M. Sasao, H. Yamaoka, M. Wada and J. Fujita, *Direct Extraction of a Na- Beam from a Sodium Plasma* ; July 1990

NIFS-36 N. Ueda, S.-I. Itoh, M. Tanaka and K. Itoh, *A Design Method of Divertor in Tokamak Reactors* Aug. 1990

NIFS-37 J. Todoroki, *Theory of Longitudinal Adiabatic Invariant in the Helical Torus*; Aug. 1990

NIFS-38 S.-I. Itoh and K. Itoh, *Modelling of Improved Confinements – Peaked Profile Modes and H-Mode–* ; Sep. 1990

NIFS-39 O. Kaneko, S. Kubo, K. Nishimura, T. Syoji, M. Hosokawa, K. Ida, H. Idei, H. Iguchi, K. Matsuoka, S. Morita, N. Noda, S. Okamura, T. Ozaki, A. Sagara, H. Sanuki, C. Takahashi, Y. Takeiri, Y. Takita, K. Tsuzuki, H. Yamada, T. Amano, A. Ando, M. Fujiwara, K. Hanatani, A. Karita, T. Kohmoto, A. Komori, K. Masai, T. Morisaki, O. Motojima, N. Nakajima, Y. Oka, M. Okamoto, S. Sobhanian and J. Todoroki, *Confinement Characteristics of High Power Heated Plasma in CHS*; Sep. 1990

NIFS-40 K. Toi, Y. Hamada, K. Kawahata, T. Watari, A. Ando, K. Ida, S. Morita, R. Kumazawa, Y. Oka, K. Masai, M. Sakamoto, K. Adati, R. Akiyama, S. Hidekuma, S. Hirokura, O. Kaneko, A. Karita, T. Kawamoto, Y. Kawasumi, M. Kojima, T. Kuroda, K. Narihara, Y. Ogawa, K. Ohkubo, S. Okajima, T. Ozaki, M. Sasao, K. Sato, K.N. Sato, T. Seki, F. Shimpo, H. Takahashi, S. Tanahashi, Y. Taniguchi and T. Tsuzuki, *Study of Limiter H- and IOC- Modes by Control of Edge Magnetic Shear and Gas Puffing in the JIPP T-IIU Tokamak*; Sep. 1990

NIFS-41 K. Ida, K. Itoh, S.-I. Itoh, S. Hidekuma and JIPP T-IIU & CHS Group, *Comparison of Toroidal/Poloidal Rotation in CHS Heliotron/Torsatron and JIPP T-IIU Tokamak*; Sep .1990

NIFS-42 T.Watari, R.Kumazawa,T.Seki, A.Ando,Y.Oka, O.Kaneko, K.Adati, R.Ando, T.Aoki, R.Akiyama, Y.Hamada, S.Hidekuma, S.Hirokura, E.Kako, A.Karita, K.Kawahata, T.Kawamoto, Y.Kawasumi, S.Kitagawa, Y.Kitoh, M.Kojima, T. Kuroda, K.Masai, S.Morita, K.Narihara, Y.Ogawa, K.Ohkubo, S.Okajima, T.Ozaki, M.Sakamoto, M.Sasao, K.Sato, K.N.Sato, F.Shinbo, H.Takahashi, S.Tanahashi. Y.Taniguchi, K.Toi, T.Tsuzuki, Y.Takase, K.Yoshioka, S.Kinoshita, M.Abe, H.Fukumoto, K.Takeuchi, T.Okazaki and M.Ohtuka, *,Application of Intermediate Frequency Range Fast Wave to JIPP T-IIU and HT-2 Plasma*; Sep. 1990

NIFS-43 K.Yamazaki, N.Ohyabu, M.Okamoto, T.Amano, J.Todoroki, Y.Ogawa, N.Nakajima, H.Akao, M.Asao, J.Fujita, Y.Hamada, T.Hayashi, T.Kamimura, H.Kaneko, T.Kuroda, S.Morimoto, N.Noda, T.Obiki, H.Sanuki, T.Sato, T.Satow, M.Wakatani, T.Watanabe, J.Yamamoto, O.Motojima, M.Fujiwara, A.Iiyoshi and LHD Design Group, *Physics Studies on Helical Confinement Configurations with l=2 Continuous Coil Systems*; Sep. 1990

NIFS-44 T.Hayashi, A.Takei, N.Ohyabu, T.Sato, M.Wakatani, H.Sugama, M.Yagi, K.Watanabe, B.G.Hong and W.Horton, *Equilibrium Beta Limit and Anomalous Transport Studies of Helical Systems*; Sep. 1990

NIFS-45 R.Horiuchi, T.Sato, and M.Tanaka, *Three-Dimensional Particle Simulation Study on Stabilization of the FRC Tilting Instability*; Sep. 1990

NIFS-46 K.Kusano, T.Tamano and T. Sato, *Simulation Study of Nonlinear Dynamics in Reversed-Field Pinch Configuration*; Sep. 1990

NIFS-47 Yoshi H.Ichikawa, *Solitons and Chaos in Plasma*; Sep. 1990

NIFS-48 T.Seki, R.Kumazawa, Y.Takase, A.Fukuyama, T.Watari, A.Ando, Y.Oka, O.Kaneko, K.Adati, R.Akiyama, R.Ando, T.Aoki, Y.Hamada, S.Hidekuma, S.Hirokura, K.Ida, K.Itoh, S.-I.Itoh, E.Kako, A. Karita, K.Kawahata, T.Kawamoto, Y.Kawasumi, S.Kitagawa, Y.Kitoh, M.Kojima, T.Kuroda, K.Masai, S.Morita, K.Narihara, Y.Ogawa, K.Ohkubo, S.Okajima, T.Ozaki, M.Sakamoto, M.Sasao, K.Sato, K.N.Sato, F.Shinbo, H.Takahashi, S.Tanahashi, Y.Taniguchi, K.Toi and T.Tsuzuki, *Application of Intermediate Frequency Range Fast Wave to JIPP T-IIU Plasma*; Sep.1990

NIFS-49 A.Kageyama, K.Watanabe and T.Sato, *Global Simulation of the Magnetosphere with a Long Tail: The Formation and Ejection of Plasmoids*; Sep.1990

NIFS-50 S.Koide, *3-Dimensional Simulation of Dynamo Effect of Reversed Field Pinch*; Sep. 1990

NIFS-51 O.Motojima, K. Akaishi, M.Asao, K.Fujii, J.Fujita, T.Hino, Y.Hamada, H.Kaneko, S.Kitagawa, Y.Kubota, T.Kuroda, T.Mito, S.Morimoto, N.Noda, Y.Ogawa, I.Ohtake, N.Ohyabu, A.Sagara, T. Satow, K.Takahata, M.Takeo, S.Tanahashi, T.Tsuzuki, S.Yamada, J.Yamamoto, K.Yamazaki, N.Yanagi, H.Yonezu, M.Fujiwara, A.Iiyoshi and LHD Design Group, *Engineering Design Study of Superconducting Large Helical Device*; Sep. 1990

NIFS-52 T.Sato, R.Horiuchi, K. Watanabe, T. Hayashi and K.Kusano, *Self-Organizing Magnetohydrodynamic Plasma*; Sep. 1990

NIFS-53 M.Okamoto and N.Nakajima, *Bootstrap Currents in Stellarators and Tokamaks*; Sep. 1990

NIFS-54 K.Itoh and S.-I.Itoh, *Peaked-Density Profile Mode and Improved Confinement in Helical Systems*; Oct. 1990

NIFS-55 Y.Ueda, T.Enomoto and H.B.Stewart, *Chaotic Transients and Fractal Structures Governing Coupled Swing Dynamics*; Oct. 1990

NIFS-56 H.B.Stewart and Y.Ueda, *Catastrophes with Indeterminate Outcome*; Oct. 1990

NIFS-57 S.-I.Itoh, H.Maeda and Y.Miura, *Improved Modes and the Evaluation of Confinement Improvement*; Oct. 1990

NIFS-58 H.Maeda and S.-I.Itoh, *The Significance of Medium- or Small-size Devices in Fusion Research*; Oct. 1990

NIFS-59 A.Fukuyama, S.-I.Itoh, K.Itoh, K.Hamamatsu, V.S.Chan, S.C.Chiu, R.L.Miller and T.Ohkawa, *Nonresonant Current Drive by RF Helicity Injection*; Oct. 1990

NIFS-60 K.Ida, H.Yamada, H.Iguchi, S.Hidekuma, H.Sanuki, K.Yamazaki and CHS Group, *Electric Field Profile of CHS Heliotron/Torsatron Plasma with Tangential Neutral Beam Injection*; Oct. 1990

NIFS-61 T.Yabe and H.Hoshino, *Two- and Three-Dimensional Behavior of Rayleigh-Taylor and Kelvin-Helmholz Instabilities*; Oct. 1990

NIFS-62 H.B. Stewart, *Application of Fixed Point Theory to Chaotic Attractors of Forced Oscillators;* Nov. 1990

NIFS-63 K.Konn., M.Mituhashi, Yoshi H.Ichikawa,*Soliton on Thin Vortex Filament;* Dec. 1990

NIFS-64 K.Itoh, S.-I.Itoh and A.Fukuyama,*Impact of Improved Confinement on Fusion Research;* Dec. 1990

NIFS -65 A.Fukuyama, S.-I.Itoh and K. Itoh,*A Consistency Analysis on the Tokamak Reactor Plasmas;* Dec. 1990

NIFS-66 K.Itoh, H. Sanuki, S.-I. Itoh and K. Tani,*Effect of Radial Electric Field on α-Particle Loss in Tokamaks;* Dec. 1990

NIFS-67 K.Sato,and F.Miyawaki,*Effects of a Nonuniform Open Magnetic Field on the Plasma Presheath*; Jan.1991

NIFS-68 K.Itoh and S.-I.Itoh,*On Relation between Local Transport Coefficient and Global Confinement Scaling Law;* Jan. 1991

NIFS-69 T.Kato, K.Masai, T.Fujimoto,F.Koike, E.Källne, E.S.Marmar and J.E.Rice,*He-like Spectra Through Charge Exchange Processes in Tokamak Plasmas;* Jan.1991

NIFS-70 K. Ida, H. Yamada, H. Iguchi, K. Itoh and CHS Group, *Observation of Parallel Viscosity in the CHS Heliotron/Torsatron* ; Jan.1991

NIFS-71 H. Kaneko, *Spectral Analysis of the Heliotron Field with the Toroidal Harmonic Function in a Study of the Structure of Built-in Divertor* ; Jan. 1991

NIFS-72 S. -I. Itoh, H. Sanuki and K. Itoh, *Effect of Electric Field Inhomogeneities on Drift Wave Instabilities and Anomalous Transport* ; Jan. 1991

NIFS-73 Y.Nomura, Yoshi.H.Ichikawa and W.Horton,*Stabilities of Regular Motion in the Relativistic Standard Map;* Feb. 1991

NIFS-74 T.Yamagishi, *;Electrostatic Drift Mode in Toroidal Plasma with Minority Energetic Particles,* Feb. 1991

NIFS-75 T.Yamagishi, *Effect of Energetic Particle Distribution on Bounce Resonance Excitation of the Ideal Ballooning Mode,* Feb. 1991

NIFS-76 T.Hayashi, A.Takei, N.Ohybu, T.Sato, *Suppression of Magnetic Surface Breaking by Simple Extra Coils in Finite Beta Equilibrium of Helical System*; Feb. 1991

NIFS-77 N.Ohyabu, *High Temperature Divertor Plasma Operation;* Feb. 1991

NIFS-78 K.Kusano, T.Tamano and T.Sato, *Simulation Study of Toroidal Phase-Locking Mechanism in Reversed-Field Pinch Plasma;* Feb. 1991

NIFS-79 K.Nagasaki, K.Itoh and S.-I.Itoh, *Model of Divertor Biasing and Control of Scrape-off Layer and Divertor Plasmas;* Feb. 1991